SF2A 2024
M. Béthermin, K. Baillié, N. Lagarde, J. Malzac, R.-M. Ouazzani, J. Richard, O. Venot, A. Siebert (eds)

COUPLING HAZE AND CLOUD MICROPHYSICS IN HOT-JUPITER ATMOSPHERES

A. Arfaux[1] and P. Lavvas[1]

Abstract. Haze and clouds are expected in many exoplanet atmospheres, demonstrating various compositions, and have been the subject of many works. However, most studies on cloud microphysics in hot-Jupiter atmospheres consider the heterogeneous nucleation of the condensing material over TiO_2 particles formed through homogeneous nucleation, whereas TiO_2 is a high temperature condensate and is not expected to form in sufficient abundances in the atmospheres we are studying, as HD-209458 b or WASP-39 b (Carone et al. 2023). In this work, we propose that photo-chemical haze particles, already expected in such atmospheres, can serve as nucleation sites, as they settle through the atmosphere. We use a cloud and haze microphysics model to compute the size distributions of hazes and condensates (as Na_2S, $MgSiO_3$ or MnS), coupled to a disequilibrium chemistry model, thus allowing to study the effect of cloud formation on the chemical composition. We first focus on the hot-Jupiter WASP-39 b, which has been observed with the JWST and we find that Na_2S, MnS and $MgSiO_3$ clouds form in the morning terminator, while the relatively higher temperature of the evening terminator allows only for $MgSiO_3$ and MnS cloud formation. The combined gas, haze & cloud composition of the two terminators provide a good fit to the JWST observations through out the spectrum, demonstrating the need for both clouds and hazes. We also conduct calculations for HD-209458b atmosphere and explore the effects of cloud formation on the thermal profile of this planet.

Keywords: haze, cloud, simulation, exoplanet, atmosphere, HD-209458 b, WASP-39 b

1 Introduction

In our precedent works (Arfaux & Lavvas 2022; Arfaux & Lavvas 2023), we found that clouds were necessary to explain the observed muted water bands for cases like WASP-39 b and HD-209458 b. Indeed, the observed water features are much weaker than those produced by our clear or hazy models, which indicates the need for additional opacities in the infrared. Such opacities can be provided by clouds obscuring the IR wavelength range. For WASP-39 b, our initial scenario is a haze-free, solar metallicity case, which provides a good fit of HST UV-visible observations (Arfaux & Lavvas 2022). However, the point of view changes with the JWST observations from Ahrer et al. (2023a,b); Alderson et al. (2023); Feinstein et al. (2023) and Rustamkulov et al. (2023). These transit observations provide further constrains on this planet's properties, especially its metallicity with a 10×Solar value which has major ramifications for the haze properties (Arfaux & Lavvas 2023). Indeed, while a solar metallicity scenario produces a Rayleigh slope in the UV that matches the observations, the larger metallicity value results in a flatter spectrum. Therefore, haze is now required to produce the necessary UV-visible slope. Similarly for HD-209458 b, our initial best-fit requires a small amount of haze to reproduce the observed UV-visible slope, but provides a rather bad fit of the IR as it does not reproduce the muted water bands. In both cases, a small amount of haze particles forms in the upper atmosphere and settles down to the deep atmosphere. In the following, we explore the possibility for these haze particles to play a role in the formation of clouds by providing adequate nuclei for heterogeneous nucleation.

2 Model

To study the formation of clouds in hot-Jupiter's atmospheres, we are relying on a 1D self-consistent model coupling haze and cloud microphysics, disequilibrium chemistry and radiative-convective transfer (Arfaux & Lavvas 2024).

[1] CNRS, Université de Reims Champagne Ardenne, GSMA, Reims, France

The disequilibrium chemistry module accounts for over a thousand reactions, including photo-chemical reactions, among more than a hundred species. To simulate photo-chemical reactions, we compute the radiation field via a radiative transfer model, assuming a disk averaged geometry. The information from the radiative model can be used to estimate the temperature profile with additional information on the intrinsic temperature and a convective scheme in the deep atmosphere. The haze microphysics part of the model accounts for the injection of a given mass flux of small haze particles in the upper atmosphere and computes the haze distribution accounting for the settling, diffusion, coagulation and sublimation of the particles, in a bin scheme. The cloud microphysics section currently accounts for tree species: Na_2S, $MgSiO_3$ and MnS. These are non-molecular condensates, nevertheless we use the classical nucleation theory considering the less abundant reactant in the surface reaction forming the condensate as a proxy. The cloud formation starts with a heterogeneous nucleation step followed by a growth via condensation, in a bin scheme. For the heterogeneous nucleation, we use the already formed haze particles as cloud condensation nuclei.

3 WASP-39 b

In the case of WASP-39 b, we choose to use fixed temperature profiles for the evening and morning terminators, derived from a GCM (Tsai et al. 2023). This method allows to account for terminator differences that can be significant for hot-Jupiter exoplanets. We explore the formation of Na_2S, $MgSiO_3$ and MnS in different haze and eddy diffusion scenarios and found a best fit with a $3 \times 10^{-15} g.cm^{-2}.s^{-1}$ haze mass flux and a nominal

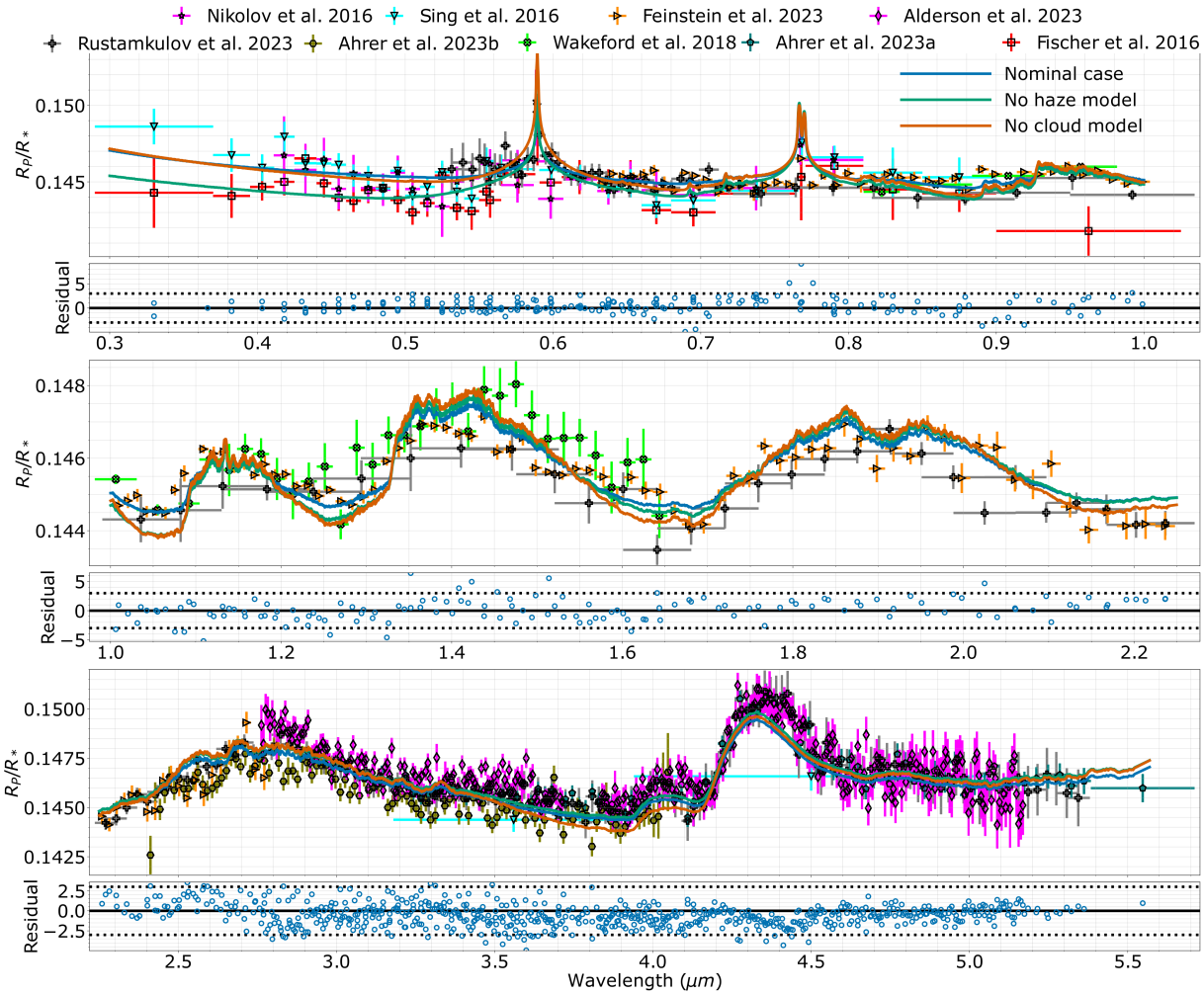

Fig. 1. Theoretical transit spectra of WASP-39 b for the nominal scenario (blue line), a haze-free case (green line) and a cloud-free case (orange). The crosses are the observations. The residuals are shown for the nominal scenario.

eddy diffusion profile derived with our parameterization (Arfaux & Lavvas 2023).

The formation of clouds on the haze particles appears to be a likely solution under the physical parameters assumed for the condensates (surface tensions: $\sigma_{Na_2S} = 100\ dyne.cm^{-1}$, $\sigma_{MgSiO_3} = 1280\ dyne.cm^{-1}$, $\sigma_{MnS} = 2326\ dyne.cm^{-1}$ and contact angle: $\theta_c = 5.7°$). An important amount of cloud effectively forms, with $MgSiO_3$ and MnS forming around 0.1 bar on both terminators and Na_2S forming above the 0.01 bar altitude and dominating the cloud distribution on the morning side. Na_2S cloud is detectable and affects the spectrum (shown in Fig. 1) resulting in a clear enhancement of the IR region with muted water bands due to cloud opacities. In addition, the small amount of haze present in the atmosphere results in the presence of a UV-visible slope matching the Hubble observations in this wavelength range. Finally, we note that the removal of sodium on the morning side, due to the formation of Na_2S, strongly reduces the strength of the Na line, providing a good match with the observations. Overall, our model including coupled haze/clouds results in a good fit of most observations along the wavelength range covered by the various VLT (Nikolov et al. 2016), HST (Sing et al. 2016; Wakeford et al. 2018) and JWST observations. It is necessary to note that most of the observed effects are coming from Na_2S condensates. Indeed, $MgSiO_3$ and MnS form deep in the atmosphere below the region probed by the transit observations in the near IR. Therefore, these species present no detectable footprint in the wavelength range under investigation. Additional observations at 10 μm could detect the silicate feature if $MgSiO_3$ is actually present in WASP-39 b's atmosphere.

4 HD-209458 b

In the case of HD-209458 b, we computes the temperature self-consistently assuming a disk averaged geometry, in order to observe how the formation of clouds can affect the thermal structure of the atmosphere. We only account for the formation of $MgSiO_3$, which is the most likely condensate expected at the pressure-temperature conditions of the atmosphere of this planet.

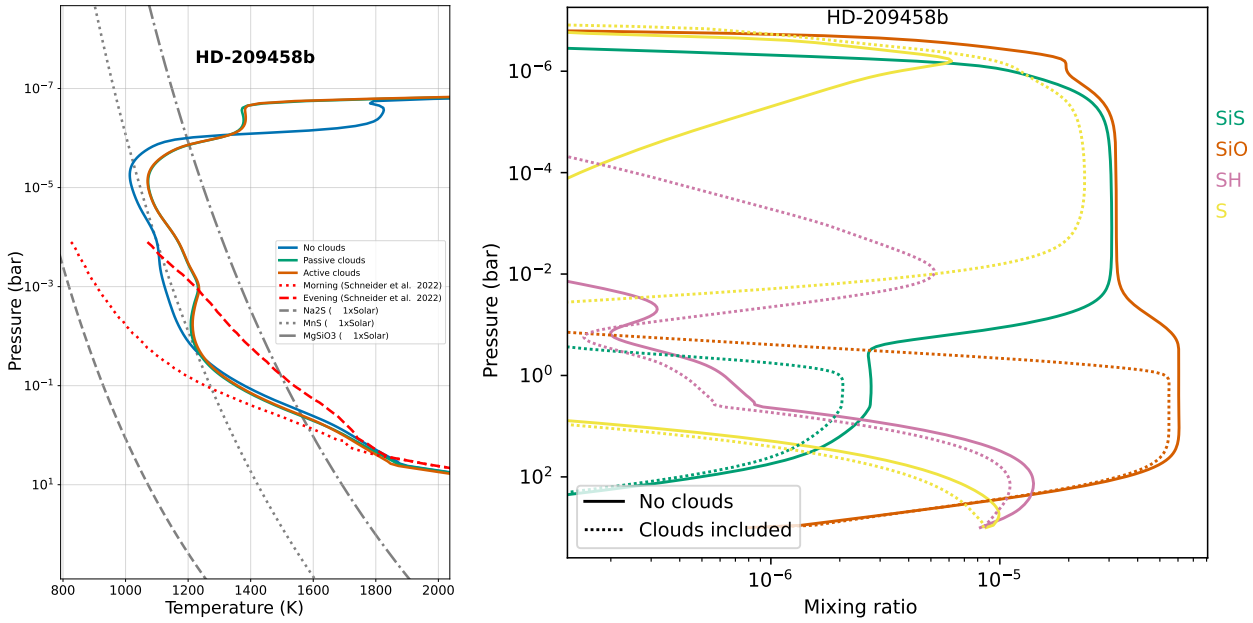

Fig. 2. Left: Self-consistent temperature profiles for HD-209458 b. The blue curve is the cloud-free case, the green and orange curves are the cloudy scenarios. For the green line, clouds are considered radiatively passive, while the orange line considers radiatively active clouds. The grey curves are condensation curve of different condensates under solar metallicity. The red curves are morning/evening temperature profiles from a GCM (Schneider et al. 2022). **Right:** Composition profiles for sulfur and silicon chemistry of HD-209458 b. The solid lines correspond to the cloud-free case and the dotted lines to the cloudy scenario.

We observe that $MgSiO_3$ forms deep in the atmosphere around 0.1 bar and therefore has week direct effects on the radiation field and the thermal structure of the planet (left panel in Fig. 2, comparing the green and orange curves). However, in comparing the no clouds (blue curve) and cloudy (green curve) scenarios, we observe

a strong effect related to how cloud formation affects the chemistry, particularly that of silicon and sulfur (right panel in Fig. 2). In the cloud-free scenario, the silicon chemistry is dominated by SiS in the upper atmosphere. Since the [Si/S] solar ratio is larger than unity, most of the sulfur is trapped in SiS which hampers the formation of other sulfur-bearing species. However, in the cloudy scenario, the silicon is depleted and cold-trapped by the formation of $MgSiO_3$, which prevents the formation of SiS in the upper atmosphere. This results in a more diverse sulfur chemistry in the upper atmosphere, with the notable formation of SH, which is radiatively active and locally heats the atmosphere leading a temperature inversion around 1 mbar.

Despite those interesting results, it is to note that the IR issue remains with still as strong water features as in the cloud-free scenario. On the possible solutions, we expect that additional cloud species can form. Considering terminator heterogeneity, it is possible in the most extreme scenario to observe the formation of Na_2S condensates on the morning side. However, that would require major terminators temperature differences (c.f. left panel in Fig. 2) and/or a metallicity over ten times the solar value, larger than the one provided by recent JWST observations (Xue et al. 2024). These conditions make that scenario unlikely. On the other hand, MnS is expected to form in HD-209458 b atmosphere and might be present high enough considering a 5×solar metallicity, which would make this condensate a possible answer to the oserved muted water bands.

5 Conclusions

Our work indicates that haze particles can serve as CCN under the right conditions and that the cloud formed this way are able to affect considerably the transit spectra. In the case of WASP-39 b, the coupling between haze and clouds provides a good fit to the observations on the whole observed wavelength range, notably the HST and JWST observations. We have also noted the importance of metallicity in understanding the haze distribution as both affects the UV-visible slope, and we highlight the importance of that parameter in haze retrievals. Finally, we have explored the implications of separating morning and evening terminators, which can present very different properties in terms of cloud composition and chemistry, with major ramifications for the transit spectrum.

In the case of HD-209458 b, we explored the radiative feedback of clouds and we observed that, despite a weak direct effect from $MgSiO_3$, the change in chemical composition due to cold traps has major implications for the radiation field and temperature structure. However, we observed that $MgSiO_3$ can not reproduce the muted water bands, and we suggest that, with a higher metallicity, other condensates like MnS or Na_2S might bring a satisfactory solution to that issue. We are planning on exploring these possibilities in a near future.

We acknowledge support from the Programme National de Planétologie (PNP) of INSU/CNRS through the project TISSAGE and from the ANR e-PYTHEAS.

References

Ahrer, E.-M., Alderson, L., Batalha, N. M., et al. 2023a, Nature, 614, 649

Ahrer, E.-M., Stevenson, K. B., Mansfield, M., et al. 2023b, Nature, 614, 653

Alderson, L., Wakeford, H. R., Alam, M. K., et al. 2023, Nature, 614, 664

Arfaux, A. & Lavvas, P. 2022, Monthly Notices of the Royal Astronomical Society, 515, 4753

Arfaux, A. & Lavvas, P. 2023, Monthly Notices of the Royal Astronomical Society, 522, 2525

Arfaux, A. & Lavvas, P. 2024, Monthly Notices of the Royal Astronomical Society, 530, 482

Carone, L., Lewis, D. A., Samra, D., Schneider, A. D., & Helling, C. 2023, WASP-39b: exo-Saturn with patchy cloud composition, moderate metallicity, and underdepleted S/O

Feinstein, A. D., Radica, M., Welbanks, L., et al. 2023, Nature, 614, 670

Nikolov, N., Sing, D. K., Gibson, N. P., et al. 2016, The Astrophysical Journal, 832, 191

Rustamkulov, Z., Sing, D. K., Mukherjee, S., et al. 2023, Nature, 614, 659

Schneider, A. D., Carone, L., Decin, L., et al. 2022, Exploring the deep atmospheres of HD 209458b and WASP-43b using a non-gray GCM

Sing, D. K., Fortney, J. J., Nikolov, N., et al. 2016, Nature, 529

Tsai, S.-M., Lee, E. K. H., Powell, D., et al. 2023, Photochemically-produced SO_2 in the atmosphere of WASP-39b

Wakeford, H. R., Sing, D. K., Deming, D., et al. 2018, The Astronomical Journal, 155, 29

Xue, Q., Bean, J. L., Zhang, M., et al. 2024, ApJ, 963, L5